Proceedings of HT-FED 2004:
2004 ASME Heat Transfer/Fluid Engineering Summer Conference
July 11-15, 2004, Charlotte, North Carolina, USA

HT-FED2004-56537

UNCERTAINTY ANALYSIS OF INFRARED THERMOGRAPHY IN CONVECTIVE HEAT TRANSFER

Nelson K. Akafuah
Carsie A. Hall, III
Ting Wang
Energy Conversion and Conservation Center
University of New Orleans
New Orleans, Louisiana

ABSTRACT

Infrared thermography is the preferred choice in many industrial processes for thermal diagnostics, condition monitoring, and non-destructive testing. However, the inherent uncertainty of surface emissivity affects the accuracy of temperature measurement by infrared thermography. In this paper a comprehensive experimental investigation was conducted to assess the uncertainty of infrared thermography in convective heat transfer. Four convective heat transfer conditions, including natural and forced convection on a flat plate, were studied. A composite test plate was constructed with an embedded heater and thermocouples. The thermocouples were used as references to compare with measurements by the infrared camera. The results indicate that the uncertainty of temperature measurement is about 4°F (2.7 % of the wall-to-ambient temperature difference) with the largest uncertainty being contributed by calibration of the infrared camera. The uncertainty of the heat transfer coefficient is 4.2% which is largely contributed by wall temperature measurement.

NOMENCLATURE

A	Plate surface area.
K	Thermal conductivity of air
K_c	Thermal conductivity of copper
K_p	Thermal conductivity of Plexiglas
Nu	Nusselt number, Equation (5)
PF	Power factor
Pr	Prandlt number
Q	Total heater power
Ra_x	Local Rayleigh number, Equation (10)
Re_x	Local Reynolds number
R_l	Shunt resistance
Ta	Non-uniformity of temperature within mapping area
T_{TC}	Mean temperature measured by thermocouple
T_{IR}	Mean temperature measured by infrared camera
T_{wTC}	Wall temperature measured by thermocouple
T_{ambTC}	Ambient temperature measured by thermocouple
$T_{Iso\ TC}$	Isothermal box temperature measured by thermocouple
T_{BPTC}	Boiling point temperature measured by thermocouple
T_{IPTC}	Ice point temperature measured by thermocouple
T_{wIR}	Wall temperature measured by infrared camera
V_L	Load voltage drop
V_R	Shunt resistance voltage drop

Greek Letters

σ	Stefan-Boltzmann constant
ε	Emissivity
ρ	Density

Subscripts:

o	Imprecision uncertainty
u	Unsteadiness uncertainty
c	Calibration uncertainty

INTRODUCTION

Infrared thermography provides a non-intrusive and remote monitoring capability for evaluating the thermal signature of an object or process to establish its performance or operating condition.

The accuracy of infrared thermography is not easy to be assessed because it is impractical to measure the emissivity of every object in the field of view and it is also difficult to determine the emissivity of a single object since surface conditions of objects (especially metals) change with time due to surface oxidation or deposition of foreign objects.

The objective of this paper is to investigate the uncertainty of emissivity variations on temperature measurement using an infrared camera and its impact on calculating heat transfer coefficient.

EXPERIMENTAL PROGRAM

The experimental setup includes a wind tunnel, a composite test wall with embedded thermocouples, a thermocouple measurement system, and an infrared camera system. There are four experimental settings, which are natural convection on a vertical flat plate, natural convection on an opened and partially enclosed horizontal flat plate, and forced convection on a vertical flat plate. The forced convection is conducted at the exit of the wind tunnel.

Test Wall

The test wall (Figure 1) is a square, composite structure, measuring 228.6 mm x 228.6 mm (9″ x 9″). It is made up of a copper plate, rubber gasket, silicone rubber heater, and Plexiglas, which are securely glued together. The Plexiglas provides structural support and is made up of four 12 mm (0.472″) thick sheets of Plexiglas glued together to form a solid wall 48 mm (1.89″) thick. This Plexiglas support wall also acts as insulation to minimize backside conduction losses. The silicone rubber heater is made of a serpentine heating element which is sandwiched between two silicone rubber sheets. The heater is rated single phase, 120 volts, 3.38 amperes, and 405.6 watts, with a power density of 5 watts/square inch. The total resistance of the heater is 35.5 ohms. Grooves are carved through the rubber gasket to accommodate and cushion the thermocouples. Twenty-four thermocouples are located in the grooves and are strategically deployed over the test surface (Figure 2). The thermocouples are 0.127 mm (36 gage) E-type thermocouple wires. The wires are insulated with Teflon and are all of the same manufacturing batch. The upper surface (test surface) of the copper plate is coated with non-glossy (flat) black paint.

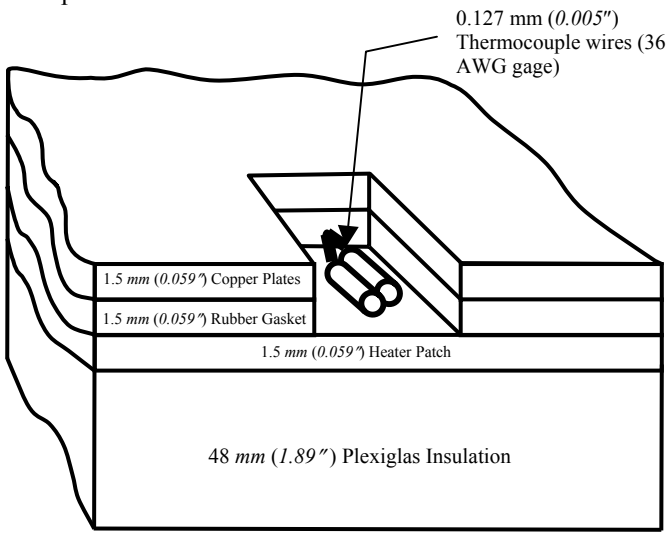

Figure 1 Cutaway Section of Test Wall

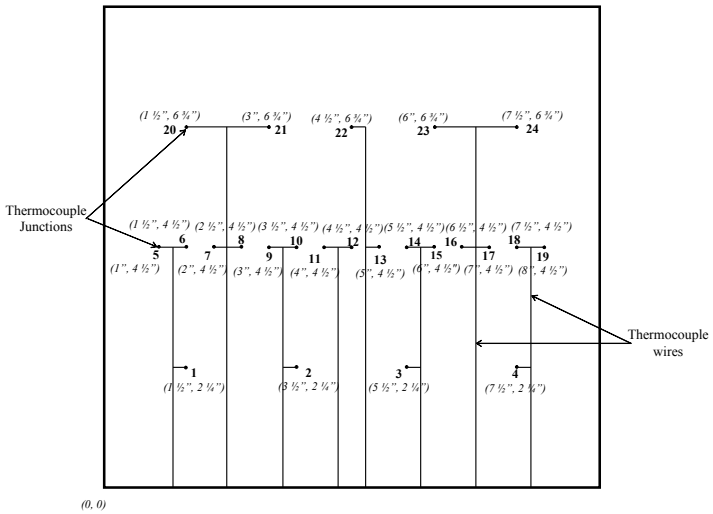

Figure 2 Thermocouple arrangements in the test surface

The Infrared Thermographic camera used is a Mikron Instrument Company's MikroScan TH7200, which is a non-contact, air cooled and high sensitive infrared radiometer. The infrared radiation emitted from the measuring object is detected and converted to an electric signal by a two-dimensional 320 x 240 uncooled focal array vanadium oxide Microbolometer. The amplified analog temperature signal is converted to a digital signal and displayed as a thermal image in color or gray scale. Each test starts after a 7-hour warm up period. Then, a series of infrared images are taken for 15 seconds. In the meantime, the thermocouple readings are taken through a Keithley 2700 Multimeter at a scan rate of 2/sec. Five data points for each thermocouple are taken.

Temperature Measurement

The infrared camera is placed 50 cm from the test surface. This gives a field of view width of 30 cm and height of 22.5 cm. The pixel size is 0.1 cm x 0.1cm. Using the pixel size and a map of the thermocouple locations, the corresponding temperature value of the infrared camera reading corresponding to each thermocouple is obtained.

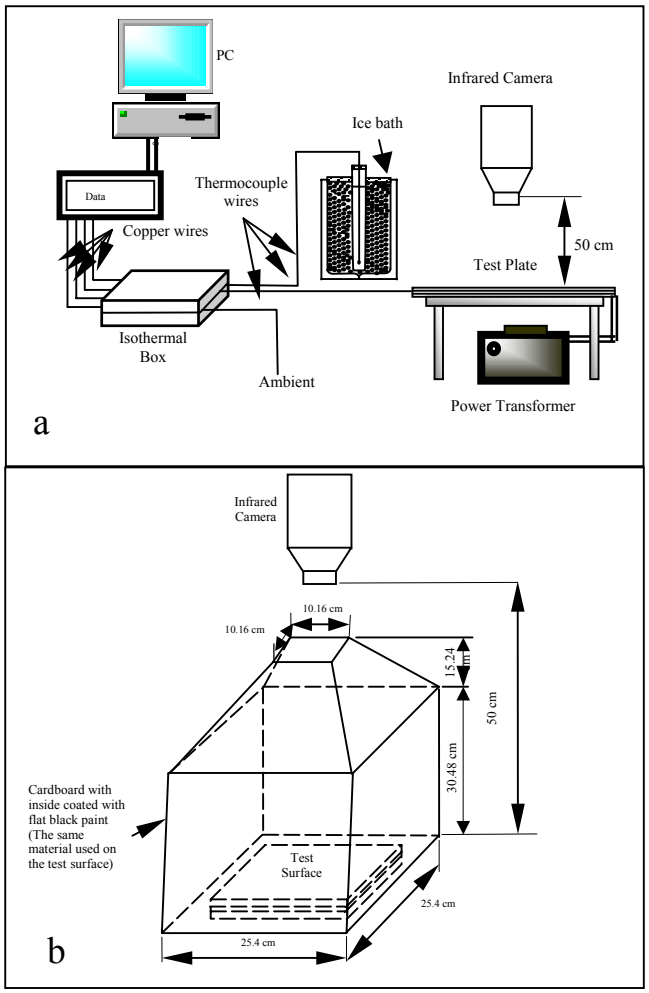

Figure 3 Schematic of experimental set up (a) horizontal flat plate, (b) partially enclosed horizontal plate

For the horizontal flat plate case, the test plate is placed horizontally as shown in Figure 3a. For the partially enclosed horizontal plate case, the test plate is placed in a partially enclosed box. The box is made of cardboard with dimensions shown in Figure 3b. The inside wall surface of the box is completely painted black with the same paint used on the test surface. This arrangement is to reduce the edge effect and ambient disturbances that will introduce background noise in the infrared image. In the vertical plate case, the plate is placed vertically, supported on a wooden stand. In the forced convection case, the test plate is placed at the exit of the wind tunnel, with the test surface parallel to the direction of the air coming out of the wind tunnel as shown in Figure 4. The free-stream velocity of the airflow at the leading edge of the test plate is 8.7 *m/s*.

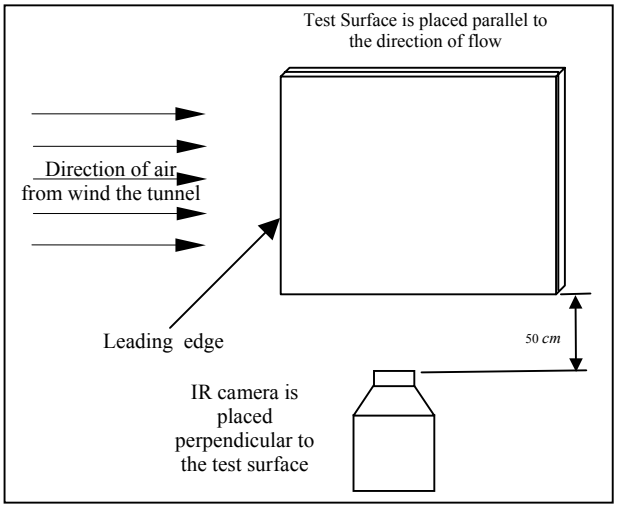

Figure 4 Schematic of the experimental set up for forced convection

UNCERTAINTY ANALYSIS

Uncertainty is not an error. For a single observation, the error is the difference between the true value and the measured value; whereas, uncertainty is the possible value that the error might take on in a given interval. The uncertainty analysis performed in this study follows the procedures laid out by Moffat [1] and ASME PTC 19-1-1985 Performance Test Code [2]. The uncertainty, or what one think the error might be, may vary considerably depending on the confidence level of the observation. A confidence level of 95 % is used in this study.

Uncertainty Analysis of Temperature Measurement

The resultant for this analysis is the difference in temperature measured using thermocouples and infrared camera.

$$\Delta T = T_{wTC} - T_{wIR} \qquad (1)$$

The two variables T_{wTC} and T_{wIR} are dependent variables, which are the resultants of other measured variables. In order to assess the uncertainty of T_{wTC} and T_{wIR}, respectively, it is necessary to backward-trace the measurement procedure until the "root" of the independent raw measurement is found, a procedure used by Wang and Simon [3]. For example, the value of T_{wTC} is measured by reading the thermocouple emf output via a digital multimeter, so at one of the terminals of "backward tracing" process is the raw voltage reading in millivolts from the multimeter. This reading is original and independent of any other readings or parameters. The backward tracing of T_{wTC} and T_{wIR} are considered separately as shown in the dashed boxes in Figures 5a and 5b. The uncertainty of ΔT is then computed from the results from the uncertainties of T_{wTC} and T_{wIR}. The variables listed outside the dash boxes are independent (or primary) measured values.

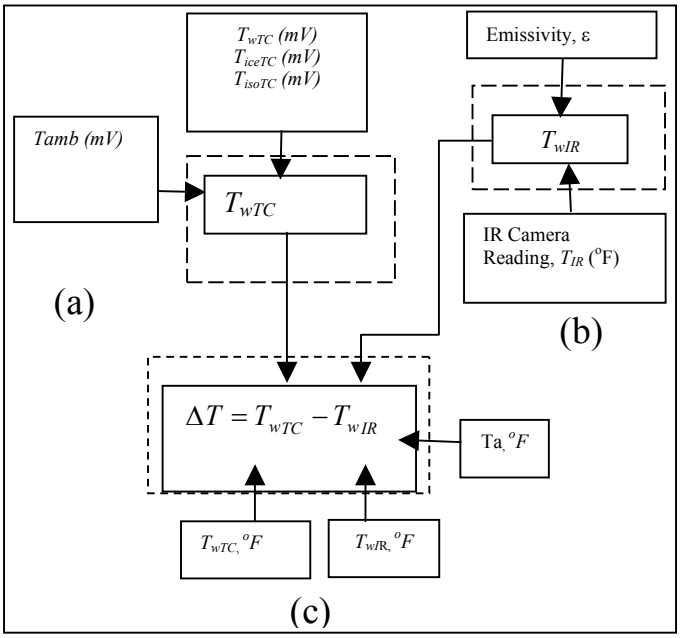

Figure 5 Block diagram illustrates the backward tracing procedure for identifying the independent variables of (a) the thermocouple readings, (b) IR readings, (c) comparing the IR readings with TC readings. The variables outside the dash boxes are independent (or primary) measured values.

In Figure 5a, the resultant T_{wTC}, dependent on several independent (or primary) variables. These variables are: $T_{\infty TC}$, T_{isoTC}, T_{BPTC}, and T_{iceTC}. In Figure 5b, the expected resultant T_{wIR} depends on two primary variables: emissivity ε of the surface and the infrared camera temperature reading, T_{IR}.

Finally, to compare the thermocouple reading with that of the infrared camera, the locations of the embedded thermocouples are mapped to the pixel locations corresponding to them. However, since there is an associated uncertainty with mapping each thermocouple to the exact corresponding pixel, a representative area, A, instead is assigned to map the thermocouples. The thermocouple is assumed to be within a mapping area, A. The standard deviation of the temperature non-uniformity in this mapping area is treated as the zeroth order uncertainty (or precision error). The uncertainty contribution of T_a and the results of the uncertainty of T_{wTC} and T_{wIR} are input into Figure 5c to compute the ΔT.

All identifiable bias errors are evaluated and removed. The random component for the instrument error is minimized by employing multiple measurements. The evaluation and removal of the known bias errors involve modeling of the process and estimation of some property values, therefore this process does not entirely remove the bias error rather it reduces the bias errors to minimal random errors, which contribute to the calibration error (N-th order). Elimination of known bias errors due to the instrument or other identifiable contributions does not exclude the possibility of some bias errors entering the experiment by other unknown means. Therefore, it is necessary to test for unknown bias errors by comparing with different measuring methods. In this study, thermocouple measurement is used for comparison. Propagation of random error components (including uncertainties in removing bias error) are computed using the technique proposed by Kline and McClintock [4]. Using this technique, the uncertainties of input independent parameters to the analysis, δX_i, all based on the same confidence interval of 95%, are combined to give a resultant uncertainty, δX_R , of the same confidence interval, as

$$\delta X_R = \left\{ \sum_i \left[\left(\frac{\partial X_R}{\partial X_i} \right) \delta X_i \right]^2 \right\}^{\frac{1}{2}} \qquad (2)$$

where $\partial X_R / \partial X_i$ is the sensitivity coefficient, which indicates

Table 1 N[th]- order uncertainty analysis for thermocouples measurements

					Nth Order		
Independent variables	Nominal values X_i	Uncertainty of imprecision $(\delta X_{i,o})$	Uncertainty of unsteadiness $(\delta X_{i,u})$	Uncertainty of calibration $(\delta X_{i,c})$	Uncertainty of Variables $(\delta X_{i,n})$	Uncertainty of Resultant δX_R (O F)	Uncertainty of Resultant $\frac{\delta X_R}{T_w - T_{amb}} x100\%$
T_{wTC}, mV	7.018	0.0005	0.0084	0.025	0.0264	0.6945	0.4437
T_{ambTC}, mV	1.400	0.0005	0.003	0.0300	0.0302	0.9077	0.5799
Total uncertainty						1.1429	0.7302

Table 2 N[th] order uncertainty analysis for infrared measurements

					Nth Order Analysis		
Independent variables	Nominal values X_i	Uncertainty of imprecision $(\delta X_{i,o})$	Uncertainty of unsteadiness $(\delta X_{i,u})$	Uncertainty of calibration $(\delta X_{i,c})$	Uncertainty of Variables $(\delta X_{i,n})$	Uncertainty of Resultant δX_R (O F)	Uncertainty of Resultant $\frac{\delta X_R}{T_w - T_{amb}} x100$
Natural convection on a vertical flat plate							
$T_{IR,}$ O F	208.9	0.05	0.0084	3.538	3.5384	3.5384	2.2606
Emissivity, ε	0.98	0.02	0.0000	0.000	0.0200	2.5510	1.6298
Total Uncertainty					3.6268	4.3621	2.7868
Natural convection on an opened horizontal flat plate							
$T_{IR,}$ O F	238.4	0.05	0.0084	4.128	4.1283	4.1283	2.6375
Emissivity, ε	0.98	0.02	0.0000	0.000	0.0200	2.8571	1.8253
Total Uncertainty					4.1284	5.0206	3.2075
Natural convection on a partially enclosed horizontal flat plate							
$T_{IR,}$ O F	242.7	0.05	0.0084	4.214	4.2143	4.2143	2.6924
Emissivity, ε	0.98	0.02	0.0000	0.000	0.0200	2.9592	1.8905
Total Uncertainty					4.2144	5.1495	3.2899
Forced convection on a vertical flat plate							
$T_{IR,}$ O F	144.9	0.05	0.0084	2.258	2.2586	2.2586	1.4429
Emissivity, ε	0.98	0.02	0.0000	0.000	0.0200	1.7708	1.1313
Total Uncertainty					2.2587	2.8700	1.8336

the sensitivity of the total resultant uncertainty to a small variation of independent parameter X_i.

This technique is also recommended by Abernathy et al [5]. The uncertainty of imprecision value, $\delta X_{i,o}$, associated with each reading, is taken to be one-half of the smallest scaled division for analog instrument and one-half of the value of the least significant digit for digital instruments. The quantitative values of precision are obtained from the manufacturer's specifications. Uncertainty of unsteadiness $\delta X_{i,u}$, associated with each reading is a measure of the unsteadiness in the measured parameter during the period of experiment. For this study five readings were recorded for each data set within a period of one minute. The unsteadiness value is the maximum deviation from the mean. The uncertainty of calibration value, $\delta X_{i,c}$, includes best estimate of uncertainties associated with the removal of identifiable bias errors (calibration and elsewhere in the facility). The uncertainty of imprecision, uncertainty of unsteadiness, and uncertainty of calibration were incorporated into the analysis by using the root mean square (rms) method, giving each variable's uncertainty contribution as

$$\delta X_{i,n} = \left[\left(\delta X_{i,o}\right)^2 + \left(\delta X_{i,u}\right)^2 + \left(\delta X_{i,c}\right)^2 \right]^{\frac{1}{2}} \qquad (3)$$

$\delta X_{i,n}$, is the Nth-order resultant uncertainty of the parameter X_i.

Since there is no simple algebraic equation to describe the relationship between independent parameters and the resultant values, a numerical perturbation method is adopted to calculate the sensitivity coefficient $\partial X_R/\partial X_i$ following Equation (4). The perturbed value ΔX_i of the nominal value X_i is given as $\Delta X_i = 0.01 X_i$ which is 1% of the nominal value. The perturbed range of X_i is given as $X_i - \Delta X_i$ and $X_i + \Delta X_i$ in Equation (4). The uncertainty of resultant in percentage is calculated based on the temperature difference between the test surface temperature and the ambient temperature as $\delta X_R/(T_w - T_{amb})$.

$$\frac{\partial X_R}{\partial X_i} = \frac{\begin{pmatrix}\text{Resultant of} \\ X_i + \Delta X\end{pmatrix} - \begin{pmatrix}\text{Resultant of} \\ X_i - \Delta X\end{pmatrix}}{2\Delta X_i} \qquad (4)$$

Uncertainty Analysis Results for Thermocouple

Two independent variables are considered in the uncertainty analysis of the thermocouple readings. The nominal value of the thermocouple reading for the test surface T_{wTC} is based on the highest emf reading of the 24 thermocouples of the entire test surface. The uncertainty of imprecision is assigned as one-half of the value of the least significant digit for the digital multimeter, which is 0.0005 *mV*. The uncertainty of unsteadiness is the maximum deviation from the mean of five reading of the thermocouples. The uncertainty of calibration, 0.025 *mV,* is computed from the evaluation of thermocouple calibration using the ice point, the boiling point of water, the isothermal box emf, and the reference table from the thermocouple manufacturer. The detailed procedure is documented in Akafuah et al [6]

The nominal value of the ambient temperature $T_{\infty TC,}$ is determined from the mean of five ambient readings. The uncertainties of imprecision and calibration are 0.005 *mV* and 0.03 *mV,* respectively. The uncertainty of unsteadiness is the maximum deviation from the mean of five ambient emf readings taken in a period of one minute. The result of the N^{th}-order analysis is shown in Table 1 for the thermocouple

Table 3 Nth- Order uncertainty analysis for matching each thermocouple location to corresponding pixels.

Independent variables	Nominal values X_i	Uncertainty of imprecision $(\delta X_{i,o})$	Uncertainty of unsteadiness $(\delta X_{i,u})$	Uncertainty of calibration $(\delta X_{i,c})$	Nth Order Uncertainty of Variables $\delta X_{i,n}$	Uncertainty of Resultant δX_R (^{O} F)	Uncertainty of Resultant % $\frac{\delta X_R}{T_w - T_{amb}} x100\%$
Natural convection on a vertical flat plate							
T_a, ^{o}F *(6x6 mm)*	208.90	0.7500	0.0084	0.0000	0.7500	0.7501	0.4792
T_a, ^{o} F*(4x4 mm)*	208.90	0.5500	0.0084	0.0000	0.5501	0.5501	0.3514
T_a, ^{o} F*(2x2 mm)*	208.90	0.2000	0.0084	0.0000	0.2002	0.2002	0.1279
Natural convection on an opened horizontal flat plate							
T_a, ^{o}F *(6x6 mm)*	238.40	1.0000	0.0084	0.0000	1.0000	1.0000	0.6389
T_a, ^{o} F*(4x4 mm)*	238.40	0.5500	0.0084	0.0000	0.5501	0.5501	0.3514
T_a, ^{o} F*(2x2 mm)*	238.40	0.4000	0.0084	0.0000	0.4001	0.4001	0.2556
Natural convection on a partially enclosed horizontal flat plate							
T_a, ^{o}F *(6x6 mm)*	242.70	1.8500	0.0084	0.0000	1.8500	1.8500	1.1819
T_a, ^{o} F*(4x4 mm)*	242.70	0.8000	0.0084	0.0000	0.8000	0.8000	0.5111
T_a, ^{o} F*(2x2 mm)*	242.70	0.7000	0.0084	0.0000	0.8000	0.7001	0.4472
Forced convection on a vertical flat plate							
T_a, ^{o}F *(6x6 mm)*	144.90	1.1000	0.0084	0.0000	1.1000	1.1000	0.7028
T_a, ^{o} F*(4x4 mm)*	144.90	0.7000	0.0084	0.0000	0.7001	0.7001	0.4472
T_a, ^{o} F*(2x2 mm)*	144.90	0.4000	0.0084	0.0000	0.4001	0.4001	0.2556

readings. The maximum uncertainty of the resultant uncertainty, 0.9077 ^oF is from the ambient temperature. The total uncertainty of the thermocouple reading is 1.1429^oF (0.7302 %). Note that the temperature values at the fourth digit after the decimal point are intentionally kept in this paper to show the values from small uncertainty contributions.

Uncertainty Analysis Results for Infrared Camera

Two independent variables are identified for the uncertainty analysis of the temperature measured by the infrared camera. The first independent parameter is the emissivity value of the paint sprayed on the test surface. The documented emissivity value for flat black paint used on the test surface is 0.96-0.98 within a temperature range of 38-93 ^oC (100-200 ^oF) [7]. It is not clear about the emissivity value higher than 200 ^{o} F, thus for this study the nominal emissivity of 0.98 is used. The uncertainty of imprecision is the value of variation in emissivity based on the best judgment of the test surface including the uncertainty of extrapolating the emissivity value at temperature higher than 200 °F, which is ± 0.02. Uncertainty of unsteadiness and calibration are presumed negligible. For the forced convection on a vertical flat plate, where the average test surface temperature is lower (144.9 ^oF), a nominal emissivity of 0.96 is used.

The second independent variable is the temperature reading, T_{IR}, of the infrared camera. The nominal value is chosen as the highest infrared camera reading of the test surface. The uncertainty of imprecision is one-half of the value of the least significant digit for reading of the camera measurement; this value is 0.05 ^{o} F. The uncertainty of unsteadiness is assigned to be the same as that indicated by the thermocouple readings because it is assumed that in the present study the unsteadiness was caused by the flow motion during the experiment, so unsteadiness is associated with the experiment not with the experiment sensors. Since the camera is new for this study, no on-site calibration is conducted in this study, and the uncertainty of calibration is based on the manufacturer's value of ± 2% of measured temperature readings in degree Celsius.

The infrared camera needs to be calibrated every two to three years of use. So in future study, the calibration error will be based on actual on-site results of calibration conducted in the laboratory. The Nth -order analysis for the infrared camera readings is shown in Table 2 for the four convective heat transfer conditions.

For all four cases, the highest contributor to the uncertainty is T_{IR} of which uncertainty of calibration is the largest uncertainty component. The accuracy of 2% of temperature value in degrees Celsius claimed by the infrared camera manufacturer is treated as the source of calibration uncertainty. The natural convection on a partially enclosed horizontal plate has the highest total uncertainty of 5.0915 ^{o} F (3.2528%). It must be noted however that the calibration uncertainty, which is ± 2 % of measured temperature in degrees Celsius, depends on the temperature value, thus the higher the temperature the higher the uncertainty value.

The forced convection case has the least uncertainty of 2.8700^oF (1.8336%). Natural convection on a vertical and horizontal plate have comparable results: 4.3621 ^oF (2.7868%) for natural convection on a vertical plate and 4.8529^oF (3.1004%) for natural convection on a horizontal plate, respectively.

Uncertainty Analysis Comparing Infrared and Thermocouple Readings

To further reduce potential unknown bias errors, the infrared measurements are compared with those measured by thermocouples. The procedure of comparison introduces uncertainty related to matching the thermocouples with the exact corresponding pixel in infrared camera. Three area sizes are chosen to evaluate uncertainty induced by position matching: 6 *mm* x 6 *mm*, 4 *mm* x 4 *mm*, and 2 *mm* x 2 *mm*. The average of all the pixel temperature reading located within the representative areas is assigned as the nominal reading. Uncertainty contribution for a variation of temperature T_a within each mapping area is computed and treated as the imprecision error. The Nth -order uncertainty analysis of T_a is shown in Table 3, for all three mapping areas and the four convective heat transfer cases.

The resultant uncertainty for all four cases show slight changes in values as the pixel area reduced. In the case of natural convection on a vertical plate the resultants uncertainties are 0.75, 0.55, and 0.20 for the areas 6 *mm* x 6 *mm*, 4 *mm* x 4 *mm*, and 2 *mm* x 2 *mm,* respectively. Smaller areas give smaller uncertainty but induce lower confidence level. The total uncertainty contribution due to mismatching the thermocouple position to the pixel is insignificant especially when compared with the largest uncertainty value contributed by the emissivity ε and the infrared camera measurement T_{IR}. Although the smaller pixel area reduces imprecision errors proportionally, the reduction is negligible in comparison with other larger errors. Therefore the large pixel area of 6 *mm* x 6 *mm* is chosen with a better confidence level (95 % confidence) without contributing to a larger overall uncertainty.

INFRARED THERMOGRAPHS

The contour plot of the infrared thermography for natural convection on a vertical plate is shown in Figure 6a. The x and y-axis in the contour plot represent pixel locations in the (x,y) spatial domain. The contour plot shows that the two-dimensional boundary layer is not fully developed, instead it shows concentric contours. This is believed to be induced by the edge effect, due to the finite size of the test plate. The contour plot for natural convection on a horizontal plate is shown in Figure 6b. The contour plot shows uniform and concentric contour lines, with lower temperature at the edges and higher temperature toward the center. This can be related to the signature of a thermal plume which develops from axisymmetric rising air.

The contour plot for natural convection on a partially enclosed horizontal plate is shown in Figure 6c. Comparing the contour plot for this case with the opened horizontal plate, the contour lines are broader, more concentric, and more centered. The enclosure clearly has minimized the edge effect and resulted to more centered concentric contours.

The contour plot for forced convection on a vertical plate is shown in Figure 7. The contours show a relatively developed boundary layer with higher temperature gradient in the direction of flow (x-direction). The contours are flatter, smoother, and narrower at the leading edge. Toward the end of the plate the contours become broader and show less temperature gradient due to growth of the boundary layer

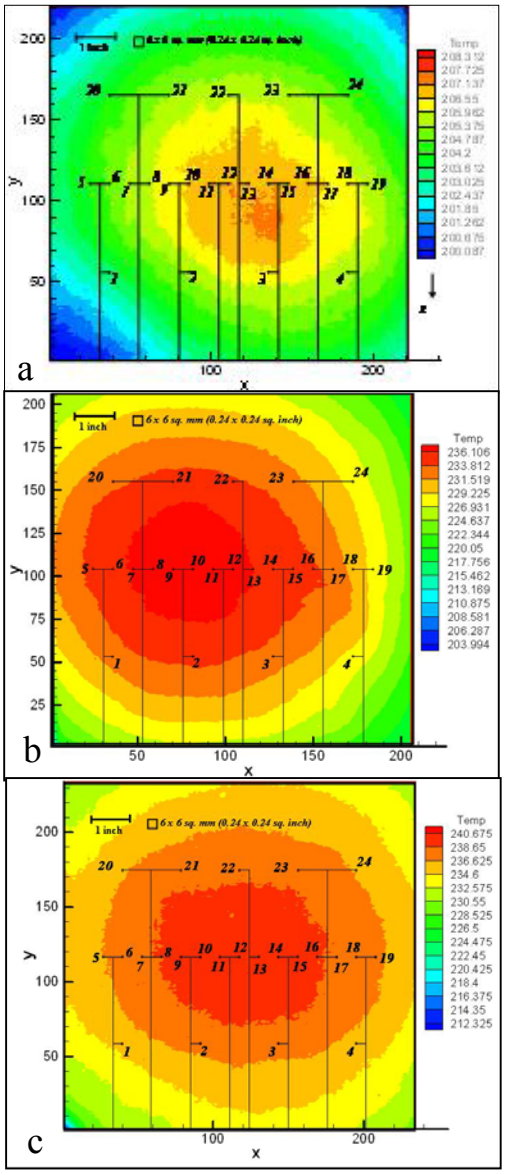

Figure 6 Thermocouple position superimposed on the thermograph for natural convection on (a) a vertical plate, (b)an opened horizontal plate, (c) a partially enclosed horizontal plate.

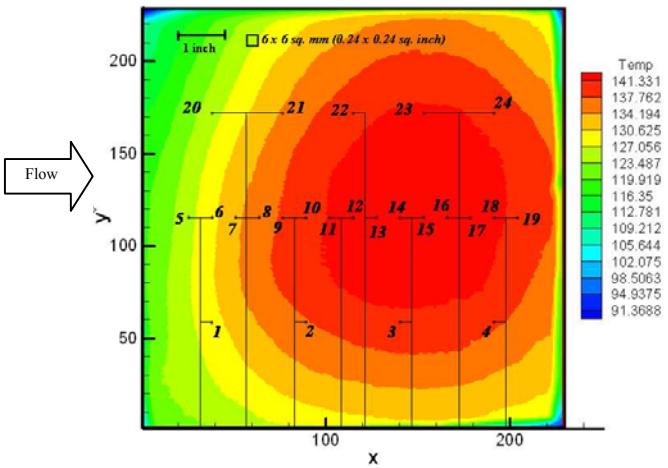

Figure 7 Thermocouple position superimposed on the thermograph for forced convection on the vertical plate

From the uncertainty analysis, the temperature difference between the infrared and thermocouple values, ΔT, for natural convection on a vertical flat plate is ± 4.572 ^{o}F; however, the individual ΔT values from 19 thermocouple measured values range from -7.151 ^{o}F to + 7.184 ^{o}F. Typically the infrared thermograph show smoother and more uniform surface temperature profile than the thermocouple measurements.

Uncertainty Analysis for Heat Transfer Coefficient

The effectiveness of heat transfer is frequently represented in terms of Nusselt number, a non-dimensional heat transfer coefficient. The local Nusselt number is given by

$$Nu = \frac{q''_w x}{K(T_w - T_{amb})} \tag{5}$$

Where, x is the characteristic length in the flow direction and q''_{net} is the net heat flux given by

$$q''_{net} = \frac{Q_{total} - Q_{cond} - Q_{Rad}}{Area} \tag{6}$$

Q_{cond} is the conduction loss from the plate, and
Q_{rad} is the radiation loss from the surface of the plate.

In conducting the uncertainty analysis for the Nusselt number, all five variables in Equation (5), except for x and T_∞ are dependent variables, which are the resultants of other measured values. A backward tracing procedure is conducted until the root (primary measured) value is found. A simplified block diagram (Figure 8) illustrates the tracking of each independent variable. The parameters considered in the uncertainty analysis of the Nusselt number are T_w, $Area$, V_R, V_L, R_I, P_F, K_p, and K_c. The uncertainty of imprecision, unsteadiness and calibration are computed from the same procedure discussed earlier. The calibration of infrared camera is in term, the largest contribution to the uncertainty of T_w. In this study, the accuracy of 2% temperature in degrees Celsius claimed by the camera manufacturer, is converted to ºF and treated as the source of calibration uncertainty. This contributes to a Nusselt number uncertainty value of 1.99 (3.54 %). The total uncertainty of Nusselt number is 2.35 (4.18 %). The black paint significantly reduces the uncertainty of emissivity, which could become a dominant source of uncertainty if the surface were left unpainted.

The local Nusselt number, Nu_x, for forced convection, is computed from Equation (7) based on uniform heat flux in a turbulent boundary layer. The turbulent convective heat transfer condition is used because the flow is tripped at the blunt leading edge of the test surface.

$$Nu_x = 0.0308\,\mathrm{Re}_x^{0.8}\,\mathrm{Pr}^{1/3} \tag{7}$$

Figure 9a shows the comparison of the experimental local Nusselt numbers computed from the infrared camera readings, thermocouples reading, and empirical correlation for the forced convection on a flat plate. The infrared results are closely consistent with the empirical result within 3 %, until the end of the plate. The deviation from the empirical value at the end of the plate can be explained as being caused by the three-dimensional edge effect because the plate has a finite width.

Figure 9b shows the comparison of local natural convection Nusselt number on a vertical plate between infrared result and

the values computed from the empirical correlation Equation (9) given by Gebhart et al [8], for laminar flow range for all values of Pr.

$$Nu_x = \frac{0.563 Ra_x^{1/4}}{\left[1+\left(\frac{0.437}{\Pr}\right)^{9/16}\right]^{4/9}} \qquad (9)$$

Where Ra_x, the Rayleigh number, is given as

$$Ra_x = \frac{g\beta(T_w - T_\infty)X^3}{\nu^2} Pr \qquad (10)$$

The infrared temperature readings are taken in the centerline along the flow direction. There is a difference of about 20% in the early part of the plate. After the middle part of the plate the difference is less than 5%. The reason could be that the test plate is finite and the edge effect affects the results as shown by the contour plot in Figure 6a.

For the horizontal flat plate, the empirical natural convection correlation (Equation (11)) for the average Nusselt number, instead of the local Nusselt for laminar flow is used for comparison as shown in Table 5.

$$\overline{Nu} = 0.15 \overline{Ra}^{1/3} \qquad (11)$$

For the partially enclosed horizontal plate, since there is no empirical correlation to compare with, it is treated as an opened horizontal plate and the empirical correlation (Equation (11)) is used for comparison. The comparison between experimental results with that of the empirical value is shown in Table 5.

For the open horizontal plate, the infrared results are within 3.25% of the empirical values, while the thermocouple results deviate 1.43% from the empirical correlation. For the partially enclosed horizontal plate, both experimental infrared and thermocouple results are lower than the empirical value for natural convection of an open horizontal plate. This is expected since the natural convection is restricted inside the enclosure.

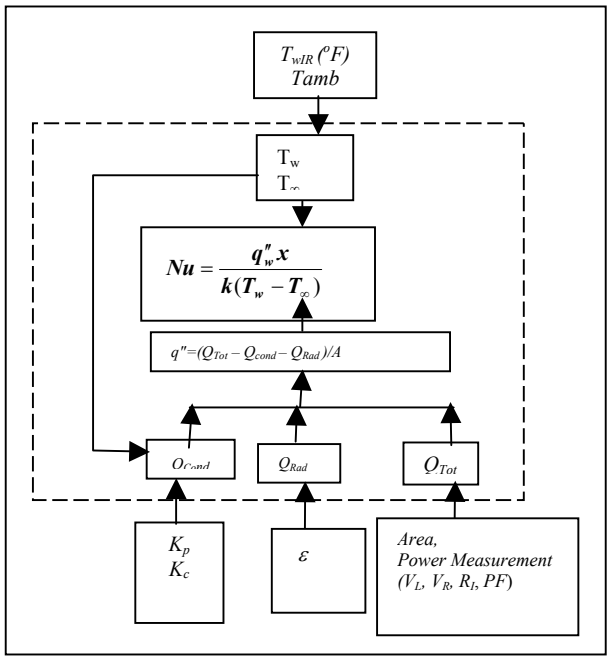

Figure 8 Block diagram illustrates the backward tracing procedure for identifying the independent variables for calculating the uncertainty analysis for the Nusselt number. Outside the dash box are independent variables.

Table 4 Nth -order uncertainty analysis for Nusselt number

					Nth Order		
Independent variables	Nominal values	Uncertainty of imprecision	Uncertainty of unsteadiness	Uncertainty of calibration	Uncertainty of variables ($\delta X_{i,n}$)	Uncertainty of resultant $\delta(Nu_x)$	Uncertainty of resultant (%) $\delta(Nu_x)/Nu_x$ x 100%
T_w (ºF)	144.9000	0.0500	0.0084	2.2580	2.2586	1.9920	3.5414
Emissivity, ε	0.9800	0.0200	0.0000	0.0000	0.0200	0.0010	0.0018
Ta_{mbTC}*,(mV)*	76.817	0.2000	0.0036	0.0300	0.2023	0.1107	0.1968
Area, (m^2)	0.0520	0.0000	0.0000	0.0000	0.0000	0.0000	0.0000
V_R*,(V)*	3.2038	0.0050	0.0700	0.1000	0.1222	0.0002	0.0004
V_L*, (V)*	57.8090	0.0050	0.7000	0.1000	0.7071	1.0397	1.8484
R_l, (Ω)	2.0000	0.0000	0.0000	0.0000	0.0000	0.0004	0.0008
PF	0.9995	0.0000	0.0080	0.0000	0.0080	0.6803	1.2095
K_p, (W/mK)	0.1875	0.0000	0.0000	0.0000	0.0000	0.0000	0.0000
Total Uncertainty (Nu_x)						2.3504	4.1785

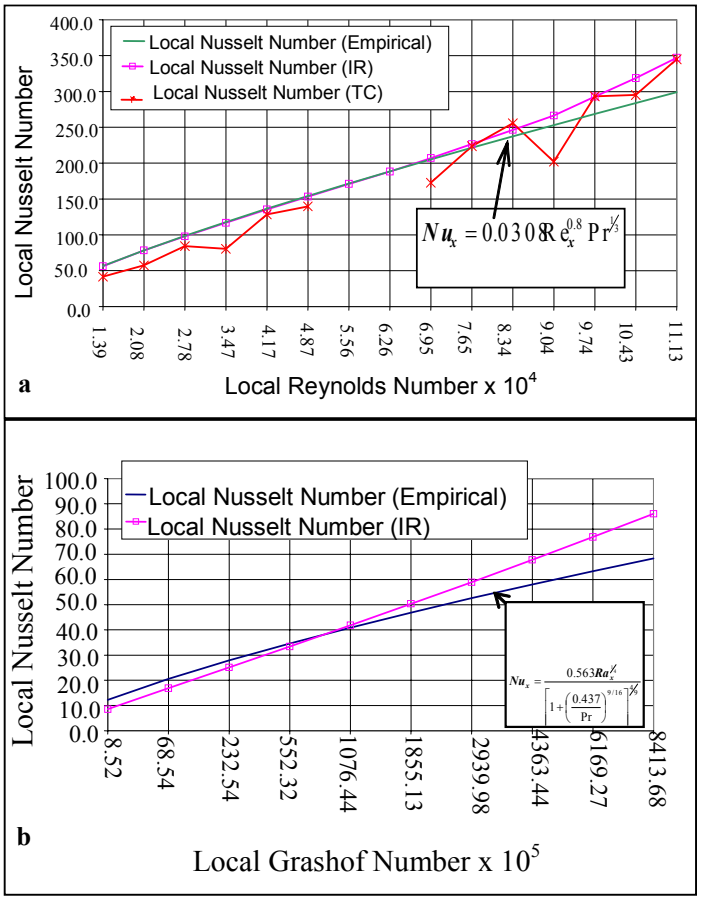

Figure 9 Nusselt number comparisons with the empirical correlations for (a) forced convection on a vertical plate (b) natural convection on a vertical plate

Table 5 Comparison of Nusselt Number between experimental and empirical correlation for Horizontal plate

Horizontal Plate	TC	IR	$\overline{Nu}$ (Empirical Results)	% Deviation (IR)	*% Deviation (TC)*
Open	74.48	71.04	73.43	3.25	1.43
Enclosed	58.48	69.20	73.90	6.36	20.86

Conclusions

This paper presents the uncertainty analysis of infrared thermography in convective heat transfer for four cases: (1) natural convection on a vertical flat plate, (2) natural convection on a horizontal flat plat, (3) natural convection on a horizontal flat within a partial enclosure and (4) forced convection on a flat plate. Thermocouple measurements were used to compare the results of the infrared thermography temperature measurements. The uncertainty contribution from the thermocouple reading, the infrared camera reading, and the pixel thermocouple matching were factored into computing the ΔT, the difference between the thermocouple and the infrared camera temperature measurements. The uncertainty analysis of ΔT gave the following resultant uncertainties: $\pm 44.37\,^{\circ}F$ *(2.79 % of* T_w-T_∞*)*, $\pm 5.02\,^{\circ}F$ *(3.21%)*, $\pm 5.15\,^{\circ}F$*(3.29%)*, and $\pm$ 2.87 $^{\circ}F$*(1.83%)* with 95 % confidence for cases 1, 2, 3, and 4 respectively. The uncertainty increases with increasing surface temperature. The largest uncertainty contribution is from the calibration error.

The uncertainty of thermocouple measurements is 1.14 ºF (0.73%). The comparison between thermocouple and IR measurements shows uncertainty within 1ºF (0.7%) for all cases except it is 1.8ºF (1.19%) for the partially enclosed horizontal plate.

The heat transfer coefficients for the various cases were computed and uncertainty analysis was performed. A bias error associated with backside heat loses and surface radiation losses were removed. The heat transfer coefficient for the forced convection was consistent with empirical result within 3%. Toward the end of the test surface, it deviated from the empirical result because of edge effect due to the finite test surface area.

The heat transfer coefficient for natural convection on a vertical plate shows consistency between the IR results and the correlations toward the center of the plate. The edge effect is seen at both ends of the test plate surface. In the case of the horizontal plates, the opened horizontal plate shows a consistent result within 3.3% for the heat transfer coefficient. An uncertainty analysis conducted on the Nusselt number for the infrared camera reading gave a total uncertainty of 2.35 (4.2 %) with 95% confidence. The largest contribution of Nu is from the surface temperature measurement.

REFERENCES

1. Moffat. R. J., "Contributions To The Theory Of Single-Sample Uncertainty Analysis" *Transaction of the ASME,* Vol. 104, June 1982, pp. 250-260.
2. Measurement Uncertainty – Instruments and Apparatus, ANSI/ASME Performance Test Code 19.1 – 1985, April 1986
3. Wang. T., and Simon. T. W., "Development Of A Special-Purpose Test Surface Guided By Uncertainty Analysis" *AIAA Journal of Thermophysics,* Vol. 3, No1, January 1989, pp. 19-25
4. Kline. S. J., and McClintock. F. A., "Describing Uncertainties in Single-Sample Experiments." *Mechanical Engineering,* January 1953, pp. 3-8.
5 Abernathy. R. B., Benedict, R.P., and Dowdell, R.B., "ASME Measurement Uncertainty," American Society of Mechanical Engineers Paper 83-WA/FM-3, Nov. 1983
6 Akafuah. N. K., Hall. C. A., and Wang. T. "Uncertainty Analysis of Infrared Thermography in Convective Heat Transfer" *ECCC Report 2003-3*, University of New Orleans.
7 Emissivity of Various Surfaces for Infrared Thermometry, Mikron Instrument Company, Inc, 2001
8 Gebhart B., Jaluria Y., Mahajan R. L., Bahgat S., *Buoyancy-Induced Flow and Transport*, Hemisphere Publishing, 1988